Laser generation of high-amplitude stress waves in materials

B. P. Fairand and A. H. Clauer
Battelle Columbus Laboratories, 505 King Avenue, Columbus, Ohio 43201
(Received 3 July 1978; accepted for publication 21 August 1978)

Stress-wave environments generated at a confined surface by a pulsed laser were investigated. Experimental measurements and theoretical calculations demonstrated that confinement of the surface with a transparent overlay provided an effective method of generating high-amplitude laser-induced stress waves in the target material. Peak pressures approaching 10 GPa were possible at laser power densities of several times 10^9 W/cm^2 for laser pulse durations ranging from several nanoseconds to several tens of nanoseconds. These pressures were generated in an air environment at standard conditions, thus enhancing their practical utilization for processing of materials and measurements of material properties. At laser power densities greater than 10^9 W/cm^2, the laser-induced stress-wave environment was controlled by properties of the ionized plasma created near the metal surface. Some enhancement in the amplitude and duration of laser-induced stress-wave environments was observed at laser power densities less than 10^9 W/cm^2 if low thermal conductivity and low heat of vaporization materials were used. Calculations show that peak pressures greater than 10 GPa were possible by superimposing stress waves either through reflection off a high acoustic impedance barrier or through the interaction of stress waves which were generated at different surfaces of a material.

PACS numbers: 79.20.Ds, 62.50.+p, 42.60.-v

I. INTRODUCTION

The generation of high-amplitude stress waves with short bursts of laser radiation was first investigated a few years after the first laser became operational.[1-4] These early studies predicted that high amplitude stress waves could be generated in materials by impinging the laser beam on an unconfined surface of the body and vaporizing a small amount of surface material. Later work which involved direct measurements of pressure showed this was not the case and peak pressures typically were less than 1 GPa.[5] Subsequently, methods to enhance the pressure environments over the free-surface conditions by modifications in the target surface conditions proved to be successful.[6-11] Our interest in this area was stimulated by the need to generate pressures greater than 1 GPa in order to produce significant changes in

the in-depth microstructures and mechanical properties of metal alloys.[12-14] A comprehensive understanding of the stress-wave environments needed to produce these changes is required for their effective application in altering the properties of materials. This paper presents our studies of laser-induced stress-wave environments with particular attention given to methods of enhancing the magnitude of the stress waves over free-surface conditions. The effects on stress-wave environments from placing transparent confining media on the target surface and addition of absorbent films to the surface are treated. Our results are based on experimental measurements of pressure and theoretical calculations using a one-dimensional radiation hydrodynamic computer code.

II. EXPERIMENTAL ENVIRONMENT AND PRESSURE-TRANSDUCER ASSEMBLIES

The experiments were performed with a CGE VD-640 Q-switched neodymium-glass laser, which consists of an oscillator followed by six amplifier stages. This system is capable of emitting up to 500 J of laser energy in a pulse that is approximately triangular in shape with a full width at half maximum of 20-40 nsec. A glass plate can be placed in the oscillator cavity to produce pulses out to approximately 100 nsec in length.

A photodiode array was used to measure the spatial profile of the laser energy emitted by the sixth amplifier. The procedure was to split off a small fraction of the laser energy and direct it to the photodiode array whose output was fed to an on-line data acquisition analysis computer system for display. Measured energy profiles have approximately a top hat configuration with considerable structure within the beam because of the high-order output mode of the oscillator-amplifier system. A 100-cm focal length convergent lens was used to focus the laser beam to the desired spot size on the target-pressure-transducer assembly. In the liquid overlay experiments, the laser beam from the last amplifier stage was directed downward by a dielectric mirror and focused onto the target. The size of the laser spot on the target was determined by directing a collinear neodynmium-YAG laser beam through the amplifier chain and measuring the spot size with an infrared viewer. Laser energy densities were defined in terms of average values over these spot sizes. Laser energy incident on target assemblies was determined by first measuring the energy at the irradiation site with a CGE carbon calorimeter. These measurements were used to standardize other carbon calorimeters which monitor the output of the laser during each shot. This monitoring was done by splitting off a small fraction of the laser energy and directing it to these on-line calorimeters.

The shape of the laser pulse emitted by the sixth amplifier was also monitored during each shot by using a beam splitter to direct a small amount of laser energy to a photodiode whose output was displayed on a fast oscilloscope. The peak laser power densities used to correlate pressure measurement results were determined by dividing the calculated average laser energy densities by the measured laser pulse full width at half maximum.

The pressures were measured with commercially available x-cut quartz crystal transducers of a shorted guard-ring design. The active elements of these gauges were right circular cylindrical disks 0.70 cm in diameter by 0.127 cm thick with an inner electrode diameter of 0.318 cm. The write time of these gauges, which is equal to a single acoustic transit time in the quartz crystal, was 222 nsec. The current output of these gauges was fed to a 50-Ω resistor and the voltage displayed on a fast oscilloscope. Over the linear range of the transducer, the pressure was calculated from the equation [15]

$$i = kA\sigma / t_o , \qquad (1)$$

where i is the current in A, A is the inner electrode area in cm^2, σ is the stress in GPa, and t_o is the transit time in μsec of a pulse through the gauge. The factor k is given by

$$k = (2.011 + 0.0107\sigma) \times 10^{-1}\ \mu C/cm^2/GPa.$$

Nonlinear effects due to conduction, changes in dielectric permittivity of the quartz, and multiple wave structure did not appear to distort the measured peak pressures up to values approaching 6 GPa. This may be due to the short duration of the laser-induced stress waves which were measured. [16]

Metal targets to measure the pressures were prepared by vacuum depositing 3-μm-thick films directly onto the front electrode surface of the quartz transducers. Some measurements also were made with targets of black paint. In these experiments, an ultraflat black Krylon paint was sprayed onto the transducer surface. The thickness of the paint coating was typically about 8-10μm. The metal and black paint coatings were covered by transparent overlays consisting of either a 2.5-cm-diam by 0.3-cm-thick disk of synthetic fused quartz or a layer of distilled water approximately 0.3 cm thick. To make the pressure measurements, the transducers were press fitted through a central hole in a 6.3-cm-diam by 1.2-cm-thick brass disk. In the water experiments, an "O"-ring was placed on the brass disk and a Lucite ring with a 2.9-cm opening centered over the transducer was pulled tightly against the brass disk with screws which were threaded into the disk. This configuration is shown in Fig. 1. The same arrangement was used in the quartz overlay experiments except the "O"-ring was placed on top of the quartz disk and the quartz was pressed against the transducer surface. In order to ensure that one-dimensional strain conditions existed in the transducer during its write time, the minimum laser spot size used in the experiments was several times the transducer inner electrode diameter.

III. THEORY OF STRESS WAVES GENERATED AT CONFINED SURFACES

A one-dimensional computer code called LILA, which is based on the method of finite differences, is used to simulate the thermal and hydrodynamic response of materials irradiated by a laser beam. The equation governing absorption of laser energy is given by

$$I = I_0(1 - R)\exp(-z\sum_i K_i), \qquad (2)$$

where I is the intensity of the absorbed energy and I_0 is the intensity of the incident laser beam. The fraction of the incident light reflected by the target is given by R.[17] The factor K_i represents the coefficient for light absorption by the i^{th} process which is summed over the different absorption processes occurring at the irradiated surface, and z is the penetration depth of the laser radiation in the material.

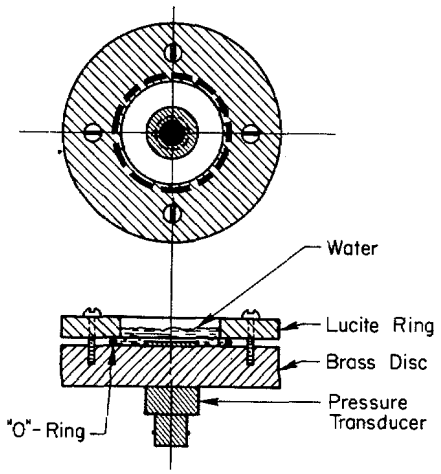

FIG. 1. Quartz transducer and holder assembly.

Absorption of laser light in metal targets is governed by two terms, K_S and K_p. One term accounts for classical absorption of electromagnetic radiation by a metallic conductor and the other term takes into account absorption in the plasma state via an inverse bremsstrahlung process.

The first term is given by [18]

$$K_s = (2\omega/C)K_I, \tag{3}$$

where K_I is the imaginary part of the complex index of refraction, w is the frequency of the incident laser radiation, and C is the velocity of light. K_I can be written in terms of the plasma frequency (w_p) of the free-electron gas in the metal and the electron-phonon collision frequency (w_c)

$$K_I = \sqrt{2}\frac{\omega}{C}\left\{\left[\left(1-\frac{\omega_p^2}{\omega^2+\omega_c^2}\right)^2+\left(\frac{\omega_p^2}{\omega^2+\omega_c^2}\right)^2\left(\frac{\omega_c}{\omega}\right)^2\right]^{1/2} - \left(1-\frac{\omega_p^2}{\omega^2+\omega_c^2}\right)\right\}^{1/2} \tag{4}$$

Temperature dependence of w_c is taken into account by a power law relation of the form T^n where n is an input parameter.

Electron-ion inverse bremsstrahlung absorption is given by Kramer's formula.[19]

$$K_p = \frac{4}{3}\left(\frac{2}{3mkT}\right)^{1/2}\frac{e^6}{hCm\nu^3}\, n_e\langle n_i z_i^2\rangle\left[1-\exp\left(-\frac{h\nu}{kt}\right)\right], \tag{5}$$

where n_e is the density of ionized electrons, n_i is the density of ions, and z_i the ionized electrons per ion. The factor ν is the frequency of the incident laser light and T is the temperature of the ionized electrons. In our problems, the electron-ion thermalization time is much shorter than the laser deposition time and electron temperature is essentially equal to the ion temperature. The remaining terms in Eq. (5) are constants for electron mass, electron charge, Boltzmann's constant, and Planck's constant.

An analytical equation of state is used to describe the behavior of a metal during irradiation by an intense beam of laser light. It is assumed that the equation of state can be formulated as a superposition of terms which separately describe the zero-temperature behavior of the material, thermal motion of heavy particles, and the thermal excitation and ionization of electrons. The zero-isotherm pressure is written as a combination of repulsive terms due to overlap of the electron shells of the positive ions and Fermi kinetic energy of the free electrons and positive ions. Thermal motion of heavy particles is represented by an interpolation equation for the free energy which, in the limit of very low densities and/or high temperatures, approaches an ideal gas equation of state. In the limit of high densities and low temperature, the interpolation relation approaches a Debye description for the material.

The internal energy and pressure terms due to excitation of the free electrons in the metal are expressed as a quadratic function of temperature, which has a limiting value equal to the Fermi degeneracy temperature (~l0^4 °K). At higher temperatures, effects due to ionization dominate. The ionized electrons are treated as an ideal gas, and the degree of ionization is determined from the solution of a set of Saha equations. The hydrodynamics are described by the standard equations of conservation of mass, momentum, and energy. Transport of thermal energy in the laser-heated material occurs by radiation diffusion using a Rosseland mean opacity approximation,[20] conduction by the metal atoms, and conduction by the ionized electrons in the plasma.[21]

IV. RESULTS OF MEASURED AND PREDICTED PRESSURE ENVIRONMENTS

Results of peak pressure measurements made with transparent quartz and water overlays and different target absorbers are shown in Fig. 2. These measurements were made in an air environment at standard conditions. The peak pressure calculated by the LILA code, which are shown as curves through

the data, are in good agreement with the experimental data. Energy losses due to reflection of laser light from the target surfaces were assumed to be small and therefore neglected in the calculations. The laser energy absorbed by the target and confined to the interaction zone is divided between internal energy in the metal/vapor, the heat of vaporization, internal energy for ionization, work done on the surrounding materials by the metal/vapor, and kinetic energy of the heated metal. Energy also thermally diffuses into the surrounding colder materials during the laser pulse, which lowers the temperature of the metal/vapor. The code predicts that a significant fraction of the absorbed energy is reradiated at the higher laser power densities. This energy, however, radiates in the vacuum ultraviolet and is trapped in the interaction zone by the overlay material.

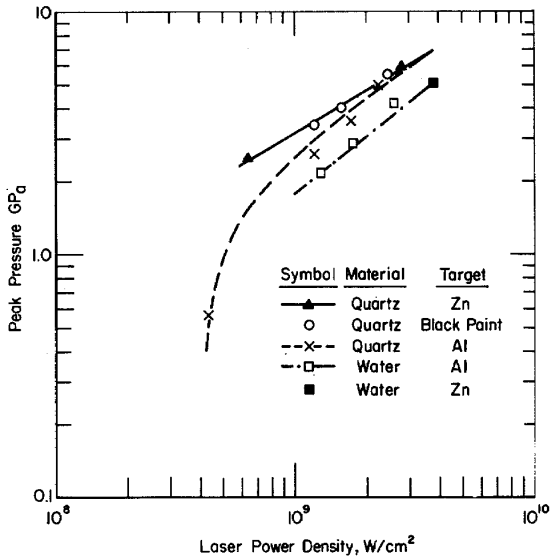

FIG. 2. Comparison of predicted and measured peak pressures generated in different target films confined by quartz or water overlays. The curves are calculated by the LILA code, the data points are experimental measurements.

As seen from Fig. 2, zinc targets covered with quartz overlays produced significantly higher peak pressures than the quartz-covered aluminum targets when the laser power density was reduced below 10^9 W/cm^2. These differences between the two pressure environments disappear by the time the laser density is increased to 4 x 10^9 W/cm^2. This behavior can be explained in the following manner. The difference in peak pressures below 1 x 10^9 W/cm^2 is due to the lower thermal conductivity of zinc compared to aluminum. In a good thermal conductor such as aluminum, a larger fraction of the absorbed laser energy thermally diffuses into the target during the laser pulse than under the same conditions with a zinc coating. This results in a lower peak temperature and thereby the lower peak pressures predicted for the aluminum targets compared to zinc coated targets. Laser-induced shock pressure measurements by Yang also suggest that a reduction in peak pressure occurs in high-conductivity materials.[9] This is noted particularly in his aluminum-and-silver target measurements. The reason the black-paint pressure measurements agree more closely with the zinc results than aluminum is attributed to the low thermal conductivity of the paint.

Earlier work reported for water overlays at laser power densities below $l0^9$ W/cm^2 exhibited a behavior similar to the quartz overlay measurements.[11] Significantly higher peak pressures were generated with zinc and black-paint targets than with aluminum. At the time of these measurements, the changes in peak pressure with target material were thought to be due to differences in surface reflectance. Based on the present work, it now appears that these differences are probably related to thermal properties of the target materials rather than reflective properties.

At laser power densities above 10^9 W/cm^2, deposition of laser energy is sufficiently intense to almost totally negate the effect of the target's thermal properties on stress-wave generation. The dense ionized plasma formed at the target surface is the dominant mechanism controlling the amplitude and duration of the stress wave. This is illustrated in Fig. 2 by the zinc-target pressure measurements made between 2 x $l0^9$ and 4 x 10^9 W/cm^2. Electron thermal conduction by ionized electrons and energy used to ionize electrons may become important at laser power densities above 4 x $l0^9$ W/cm^2. Also, at laser power densities above 4 x $l0^9$ W/cm^2, reflection of laser light by the dense surface plasma and/or optical breakdown of the transparent overlay is expected to ultimately limit the magnitude of stress waves which can be generated at target surfaces confined by transparent overlays. Neither effect appears to be a limiting factor in stress-wave generation for incident laser power densities up to 4 x $l0^9$ W/cm^2.

Based on the measured and predicted pressure environments shown in Fig. 2, the acoustic impedance of the overlay material was much less effective in changing peak pressure than the square-root dependence predicted by Anderholm in his earlier analysis.[5] Over the range of laser power densities extending from 6 x $l0^8$ W/cm^2 up to 4 x $l0^9$ W/cm^2, peak pressures for quartz and water overlays only differ by about $\sqrt{2}$. This is not surprising since the dependence of pressure on the square root of the acoustic impedance assumes the overlay and target material have the same acoustic impedance, whereas the impedance of water is approximately a factor of 10 less than aluminum or quartz. The ability to generate high peak pressures with a low-impedance liquid such as water is quite desirable, particularly in laser shock processing applications on nonplanar surfaces where multiple shocking of a single area of material is required.

The time behavior of the stress wave was controlled by the temperature of the laser-heated metal/vapor. At laser power densities above 1 x 10^9 W/cm^2, calculations predicted that most of the absorbed energy initially was used to heat this metal/vapor. For this reason, the shape of the stress wave closely followed the shape of the laser pulse until the laser pulse began to decay. The decay time of the stress wave was much slower because it was governed by the rate at which work was done on surrounding materials and the rate at which heat was conducted out of the metal/vapor into the colder adjacent materials. Experimental measurements of pressure confirmed this type of behavior. This is illustrated in Fig. 3, which compares the measured time history of the laser pulse with the measured and predicted

pressure pulse for the case of a transparent water overlay on aluminum.

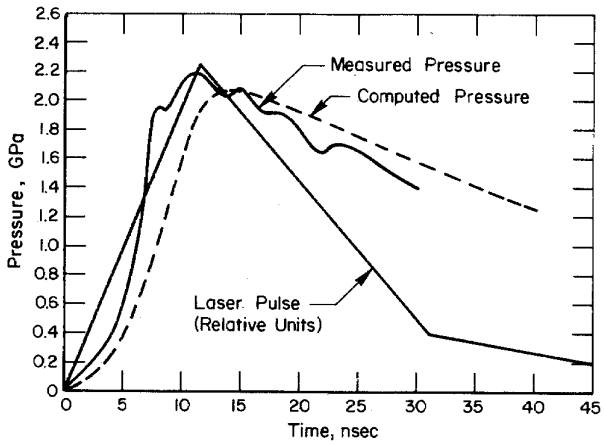

FIG. 3. Comparison of computed and measured pressures-water overlay/-aluminum target at 1.2×10^9 W/cm^2.

For laser power densities below l x l0^9 W/cm^2, it was found that the heat of vaporization of the target material can become a significant fraction of the total absorbed energy. For this reason, it is desirable to pick a material with a low heat of vaporization. Lead is a good example of such a material, as are zinc and black paint. In another paper, we looked at the effect of using lead coatings to increase the amount of plastic deformation introduced in Fe-3 wt% Si specimens.[13] More deformation was observed in the lead-coated iron specimens than in the bare iron. Computer calculations showed that the presence of lead significantly increased the duration of the high-pressure portion of the pulse compared to the bare-iron configuration. This is illustrated in Fig. 4. The longer duration stress wave generated in a lead-coated target is expected to increase the amount of shock-induced deformation, which was the result observed in the Fe-3 wt% Si experiments.[13]

V. OTHER METHODS OF ENHANCING PRESSURE ENVIRONMENTS

An acoustic impedance mismatch technique and superposition of stress waves were investigated to determine methods for generating peak pressures greater than 10 GPa. The target material selected in this study was titanium since our work with titanium requires peak pressures above 10 GPa.

The acoustic impedance mismatch technique involved placing a thin foil of the target material in intimate contact with a much higher-acoustic-impedance backup block. The principle behind this technique involved reflection of the stress wave in the titanium as a compressive pulse off the high acoustic-impedance barrier at the back surface of the titanium. This produces constructive interference and thereby enhancement in the stress-wave amplitude of the reflected stress wave in the titanium. Tungsten, which has an acoustic impedance of 7.61 x 10^6 g/cm^2 sec compared to a value of 2.11 x 10^6

g/cm^2 sec for titanium, was selected for this purpose. The configuration which was studied consisted of a 0.025-cm-thick titanium target covered with a 0.3-cm-thick quartz disk and backed by a 0.6-cm-thick tungsten disk. Results describing the material response of these experiments will be reported in a laser publication. LILA calculations of the pressure environment generated with this setup were made and an example of these calculations is shown in Fig. 5. As seen from Fig. 5, pressures greater than 10 GPa can be generated at the titanium/tungsten interface even though the pressure at the surface of the titanium is only about 6 GPa. Higher pressures than those shown in Fig. 5 can be generated by increasing the laser power density above 3 x l0^9 W/cm^2.

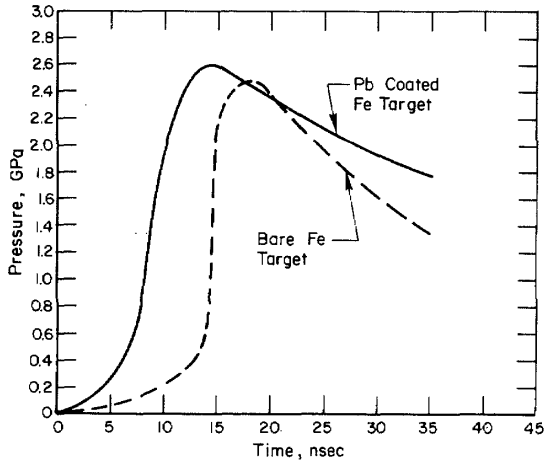

FIG. 4. Comparison of computed pressures in iron target and lead-coated iron target with quartz overlays at 6×10^9 W/cm^2.

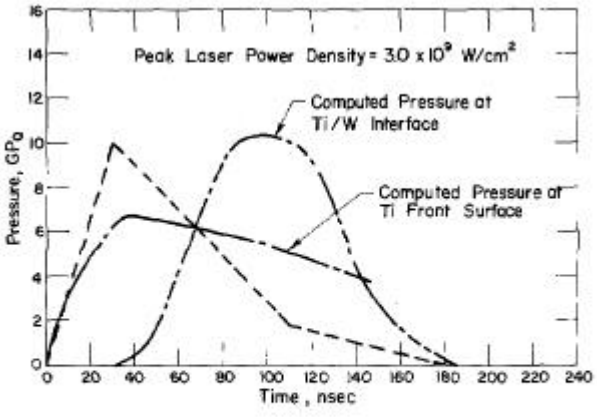

FIG. 5. Comparison of computed and measured pressures for the quartz overlay/titanium target/tungsten backup arrangement. Note: Dashed curve illustrates the shape of the laser pulse used in these calculations.

In the stress-wave superposition studies, two laser beams were allowed to simultaneously impinge on the two opposite surfaces of a thin titanium foil. The stress waves generated at each surface superimpose

near the center of the foil to generate a peak pressure approximately double that in the individual waves. From an experimental standpoint, this is quite easy to do with a laser since it only involves using a beam splitter to divide the output beam of the laser into two approximately equal parts and directing these beams simultaneously onto the opposite surfaces of the target. An example of the stress-wave environment which can be generated in this manner is shown in Figs. 6 and 7. The target consisted of a 0.025-cm-thick titanium foil covered with 0.3-cm-thick synthetic fused-quartz disks. As seen from Figs. 6 and 7, pressures greater than 10 GPa can be generated by this technique.

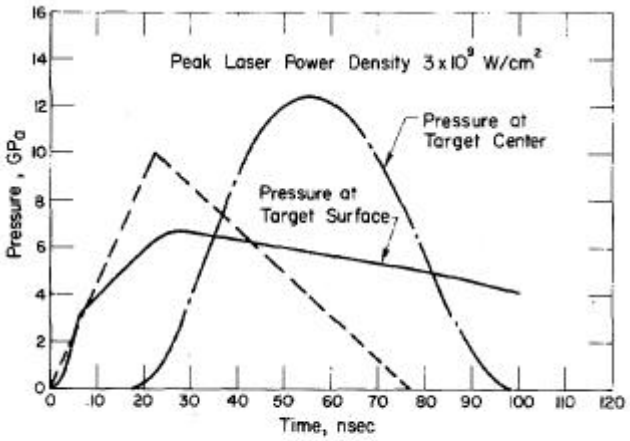

FIG. 6. Computed pressures for the split-beam configuration and the quartz overlay/0.025-cm-thick titanium target/quartz overlay arrangement. Note: Dashed curve illustrates the laser pulse shape used in these calculations.

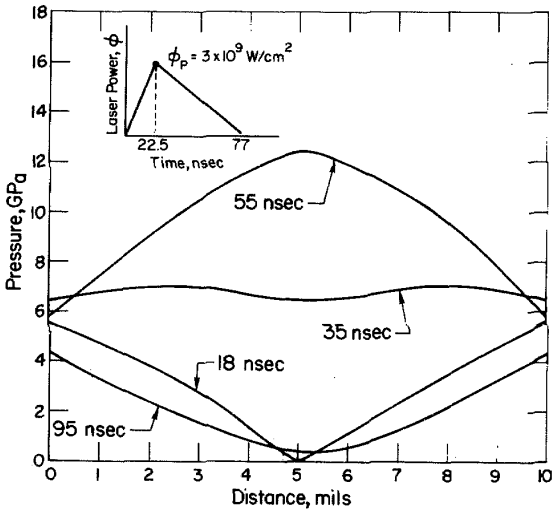

FIG. 7. Computed pressure profiles through the specimen thickness at increasing time intervals after the start of laser irradiation for the split-beam configuration and the quartz overlay/0.025-cm-thick titanium target/-quartz overlay arrangement.

VI. CONCLUSIONS

Experimental measurements and theoretical calculations demonstrated that confinement of a metal surface with a transparent overlay provided an effective method of generating high-amplitude laser-induced stress waves in the target material. Peak pressures approaching 10 GPa were possible at laser power densities of several times 10^9 W/cm^2 for laser-pulse durations ranging from several nanoseconds to several tens of nanoseconds. These pressures were generated in an air environment at standard conditions, thus enhancing their practical utilization for processing of materials and measurements of material properties.

At laser power densities greater than 10^9 W/cm^2, the laser-induced stress-wave environment was controlled by properties of the ionized plasma created near the metal surface. Some enhancement in the amplitude and duration of the laser-induced stress-wave environment was observed at laser power densities less than 10^9 W/cm^2 if low thermal conductivity and low heat of vaporization materials were used. Coating of the metal surface with such materials has the added feature of protecting the metal surface from laser melting and vaporization. Lead, zinc, and black paint were found to be effective surface coatings. Of these three materials, black paint was the most practical and can be used over the entire range of laser power densities which were investigated either to enhance the pressure environment at the lower laser power densities, or simply to protect the metal surface from melting and vaporization.

Calculations show that peak pressures greater than 10 GPa were possible by superimposing stress waves either through reflection off a high-acoustic-impedance barrier or through the interaction of stress waves which were generated at different surfaces of the material.

ACKNOWLEDGMENTS

The help of B. Campbell in assisting with the laser experiments is hereby acknowledged. This program was supported by the National Science Foundation on Grant No. DMR-72-03277 and the Army Research Office on Grant No. DAHCO4-75-G-0115.

1 G.A. Askar'yan and E.M. Moroz, JETP Lett. **16**, 1638 (1963).
2 R.M. White, J. Appl. Phys. **34**, 2123 (1963).
3 David W. Gregg and Scott J. Thomas, J. Appl. Phys. **37**, 2787 (1966).
4 C.H. Skeen and C.M. York, J. Appl. Phys. **12**, 369(1968).
5 J.D. O'Keefe and C.H. Skeen, J. Appl. Phys. **44**, 4622 (1973).
6 N.C. Anderholm, Appl. Phys. Lett. **16**, 1133 (1970)..
7 J.D. O'Keefe and C.H. Skeen, Appl. Phys. Lett. **21**, 464 (1972).
8 Jay A. Fox, Appl. Phys. Lett. **24**, 461 (1974).
9 L.C. Yang, J. Appl. Phys. **45**, 2601(1974).

[10] B.P. Fairand, A.H. Clauer, R.G. Jung, and B.A. Wilcox, Appl. Phys. Lett. **25**, 431 (1974).
[11] B.P. Fairand and A.H. Clauer, Opt. Commun. **18**, 588 (1976).
[12] B.P. Fairand, B.A. Wilcox, W.J. Gallagher, and D.N. Williams, J. Appl. Phys. **43**, 3893 (1972).
[13] A.H. Clauer, B.P. Fairand, and B.A. Wilcox, Metall. Trans. A **8a**, 119 (1977).
[14] Allan H. Clauer, Barry P. Fairand, and Ben A. Wilcox, Metall. Trans. A **8a**, 1872 (1977).
[15] R.A. Graham, F.W. Neilson, and W.B. Benedick, J. Appl. Phys. **36**, 1775 (1965).
[16] R.A. Graham and L.C. Yang, J. Appl. Phys. **46**, 5300 (1975).
[17] The standard expression for reflection of electromagnetic radiation by a metallic surface is not valid at the high laser power densities of interest in our material shock processing studies. Instead, *R* is governed by a complex interaction mechanism which substantially reduces the value of *R* below its classical value.
[18] V.L. Ginzburg, *The Propagation of Electromagnetic Waves in Plasmas* (Addison-Wesley, Reading, Mass., 1964).
[19] Ya. B. Zel'dovich and Yu. P. Raizer, *Physics of Shock Waves and High Temperature Phenomena* (Academic, New York, 1966), Vol. I, p.259.
[20] John W. Bond, Jr., Kenneth M. Watson, and Jasper A. Welch, Jr., *Atomic Theory of Gas Dynamics* (Addison-Wesley, Reading, Mass., 1965), p.371.
[21] Lyman Spitzer, Jr., *Physics of Fully Ionized Gases* (Interscience, New York, 1967), p.143.